




# Using ultrasound radiomics analysis to diagnose cervical lymph node metastasis in patients with nasopharyngeal carcinoma

Min Lin<sup>1</sup> · Xiaofeng Tang<sup>1</sup> · Lan Cao<sup>1</sup> · Ying Liao<sup>1</sup> · Yafang Zhang<sup>1</sup> · Jianhua Zhou<sup>1</sup> 

Received: 19 May 2022 / Revised: 30 July 2022 / Accepted: 18 August 2022 / Published online: 7 September 2022  
© The Author(s), under exclusive licence to European Society of Radiology 2022

## Abstract

**Objective** This study aimed to explore the clinical value of ultrasound radiomics analysis in the diagnosis of cervical lymph node metastasis (CLNM) in patients with nasopharyngeal carcinoma (NPC).

**Methods** A total of 205 cases of NPC CLNM and 284 cases of benign lymphadenopathy with pathologic diagnosis were retrospectively included. Grayscale ultrasound (US) images of the largest section of every lymph node underwent feature extraction. Feature selection was done by maximum relevance minimum redundancy (mRMR) algorithm and multivariate logistic least absolute shrinkage and selection operator (LASSO) regression. Logistic regression models were developed based on clinical features, radiomics features, and the combination of those features. The AUCs of models were analyzed by DeLong's test.

**Results** In the clinical model, lymph nodes in the upper neck, larger long axis, and unclear hilus were significant factors for CLNM ( $p < 0.001$ ). MRMR and LASSO regression selected 7 significant features for the radiomics model from the 386 radiomics features extracted. In the validation dataset, the AUC value was 0.838 (0.776–0.901) in the clinical model, 0.810 (0.739–0.881) in the radiomics model, and 0.880 (0.826–0.933) in the combined model. There was not a significant difference between the AUCs of clinical models and radiomics models in both datasets. DeLong's test revealed a significantly larger AUC in the combined model than in the clinical model in both training ( $p = 0.049$ ) and validation datasets ( $p = 0.027$ ).

**Conclusion** Ultrasound radiomics analysis has potential value in screening meaningful ultrasound features and improving the diagnostic efficiency of ultrasound in CLNM of patients with NPC.

## Key Points

- Radiomics analysis of gray-scale ultrasound images can be used to develop an effective radiomics model for the diagnosis of cervical lymph node metastasis in nasopharyngeal carcinoma patients.
- Radiomics model combined with general ultrasound features performed better than the clinical model in differentiating cervical lymph node metastases from benign lymphadenopathy.

**Keywords** Nasopharyngeal carcinoma · Lymph node metastasis · Ultrasound · Radiomics analysis

## Abbreviations

CEUS	Contrast-enhanced ultrasound
CLN	Cervical lymph node
CLNM	Cervical lymph node metastasis
ENS	Extranodal neoplastic spread

ICC	Interclass correlation coefficient
LASSO	Least absolute shrinkage and selection operator
mRMR	Maximum relevance minimum redundancy
NPC	Nasopharyngeal carcinoma
RLN	Retropharyngeal lymph node
ROC	Receiver operating characteristic
ROI	Region of interest
SWE	Shear wave elastography

✉ Jianhua Zhou  
zhoujh@sysucc.org.cn

<sup>1</sup> Department of Ultrasound, Sun Yat-Sen University Cancer Center, State Key Laboratory of Oncology in South China, Collaborative Innovation Center for Cancer Medicine, Guangdong Key Laboratory of Nasopharyngeal Carcinoma Diagnosis and Therapy, No. 651 Dongfeng Road East, Guangzhou 510060, Guangdong, People's Republic of China

## Introduction

Nasopharyngeal carcinoma (NPC) is a highly epidemiological cancer in South China [1]. It has a high incidence of cervical

lymph node metastasis (CLNM) [2]. The metastasis status of cervical lymph nodes (CLN) not only influences the NPC staging but also affects the treatment planning [3, 4]. The current magnetic resonance imaging (MRI) diagnosis criteria for CLNM of NPC include lymph node minimum diameter, central necrosis or rim enhancement, nodal grouping, and extranodal neoplastic spread (ENS), which are factors associated with prognosis [5, 6]. MRI detects metastatic lymph nodes at high efficiency [7]. The sensitivity and specificity of MRI in CLNM diagnosis were 0.88 and 0.95, respectively [8]. However, in interpreting MR images of NPC, lymph nodes of borderline size, without nodal necrosis or ENS, always poses a diagnostic challenge to the radiologist.

Ultrasound is a useful imaging modality in the evaluation of cervical lymphadenopathy because of its high sensitivity and specificity [9]. Compared with MRI, ultrasound examination is more convenient, affordable, and available. US was proved to be superior to other imaging modalities in detecting CLNM in squamous cell carcinoma of the head and neck and thyroid cancer [10–12]. US is widely used in the examination of NPC CLN. New techniques like shear wave elastography (SWE), and contrast-enhanced ultrasound (CEUS) further enhanced the efficiency of US in the diagnosis of NPC CLNM. The AUCs were 0.879 and 0.776, respectively [13, 14]. Although malignant lymph nodes are mostly accompanied by rounded shape, unsharp margin, homogenous echotexture, cortical thickening, unclear hilus structure, and necrosis, these characteristics can also be found in benign lymph nodes including tuberculosis, reactive lymphoid hyperplasia, and granulomatous inflammation [15, 16]. This hinders the identification of lymph node metastasis and benign lymphadenopathy. In the meantime, US diagnosis relies on the experience of doctors and this may lead to subjectivity. A more efficient and highly objective method is needed.

Radiomics is a method that extracts hundreds of features from medical images using data-characterization algorithms and builds algorithm models via machine learning or deep learning, which is helpful for the objective interpretation of tumor features [17]. It can quantitatively extract and analyze the features of US images by pixel level to identify the tumor information that can't be macroscopically recognized [18]. The objective characteristics of radiomics endow it with great value in diagnosing many diseases, such as thyroid cancer, lung cancer, liver cancer, and breast cancer [19–22]. This indicates a great potential usage of radiomics in the field of CLNM prediction.

The present study aimed to evaluate whether texture features extracted from grade scale ultrasound images of cervical lymph nodes could be used to improve the efficiency of US in the diagnosis of CLNM in patients with NPC.

## Materials and methods

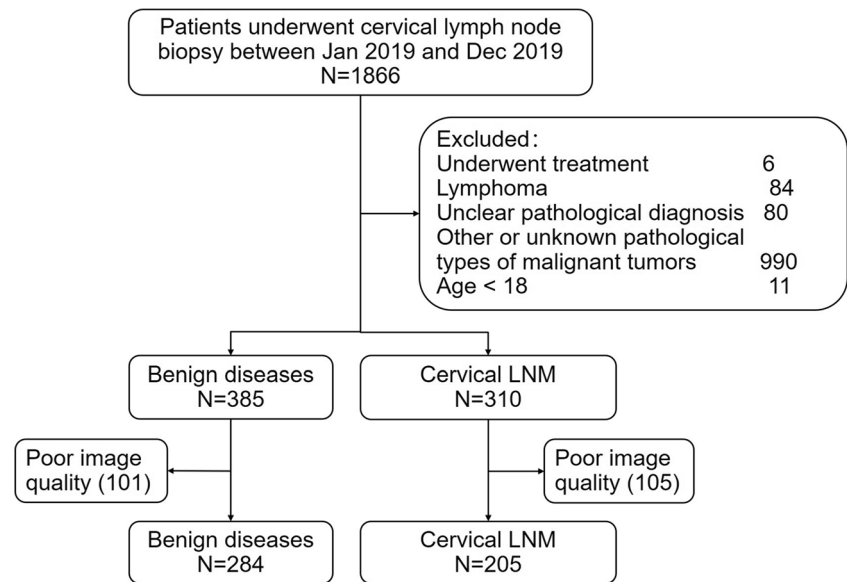
### Study population

The Institutional Review Board of Sun Yat-Sen University Cancer Center approved this study. Patients who underwent core-needle biopsy in 2019 in our hospital were investigated. NPC patients with clinically palpable enlarged cervical lymph nodes or enlarged impalpable CLN revealed by MRI received ultrasound examination, and lymph nodes with suspicious ultrasound signs would undergo a biopsy. Those pathologically diagnosed as NPC CLNM were enrolled as a positive group. For the negative group, it would be best if cervical lymph nodes with pathological diagnoses in NPC patients were enrolled. However, the first-line treatment of nasopharyngeal carcinoma is radiotherapy, and lymph node dissection is rarely performed in NPC patients. Benign lymph nodes of NPC patients rarely have pathological diagnoses. Therefore, we enrolled lymph nodes that underwent biopsy during the same period and were pathologically confirmed to be benign as the negative group instead. Patients were excluded from this study in the following conditions: age < 18, lymph node too large to be completely shown in the graph, or markers inside the lymph node (Fig. 1).

### Ultrasound image acquisition and general ultrasound characteristics collection

All included patients were evaluated by an ultrasound doctor with at least 5-year experience to determine the target lymph node for biopsy. The ultrasound examination was performed using Mindray Rezon 7T, Esaote MyLab Twice, and Hitachi ALOKA ultrasound system with a 6–15L linear array probe. Each patient was placed in the supine position while lying on the examination bed and was told to breathe calmly. The neck was fully extended during the examination. General US features such as lymph node location, size, lymph node morphology, boundary, and internal echogenicity were observed and recorded. The location (level) of the target lymph node was recorded according to the American Head and Neck Society and the American Academy of Otolaryngology-Head and Neck Surgery [23]. The cross-section size is considered the most useful radiologic criterion for assessing CLNM [24]. Therefore in this research, the US images of the largest cross-section were investigated. The size of the lymph node was recorded as long axis length and short axis length at the largest section. One grayscale US image of the target lymph node at the largest section was collected from every patient for the radiomics analysis. Demographic characteristics such as gender and age of the patients were collected.

**Fig. 1** Flow chart of patient enrollment



### Region of interest segmentation and extraction of radiomics features

Manual segmentation of the ROI was performed by 2 radiologists (with 2 years and 6 years of experience in ultrasound, respectively). Reader A segmented the ROIs twice with a 6-week interval. Reader B reviewed the ROIs drawn by reader A. When different opinions were presented between two readers, the final ROI would be determined after discussion. All ROIs were segmented on grayscale images with Artificial Intelligence Kit software (GE Healthcare) (Fig. 2). Radiomics features including first-order features, shape features, and textural features were included. From every lymph node, 386 texture features were extracted. Interobserver agreements of extracted features were determined by calculating the intraclass correlation coefficients (ICC).

### Data preprocessing

The dataset was randomly assigned in a 7:3 ratio to either the training dataset or validation dataset. All cases in the training dataset were used to train the predictive model, while cases in the validation dataset were used to independently evaluate the model's performance. Before analyses, variables with zero variance were excluded from analyses. Then, the missing values and outlier values were replaced by the median. Finally, the data were standardized by standardization.

### Feature selection and machine learning model

Logistic models were built from the training dataset and used the validation dataset to validate the model. The clinical model

was built from gender, age, and general US features. Features with a  $p$  value < 0.05 in the univariate logistics regression analysis were put into multivariate logistics regression analysis. Those with a  $p$  value < 0.05 were thought to be important factors in the diagnosis of malignancy.

The radiomics model was a logistic model built from radiomics features. Stability analysis of radiomics features was performed by removing the features with low reproducibility (ICC < 0.75). The remaining significant features were ranked using the maximum relevance minimum redundancy (mRMR) algorithm. MRMR is a filter-type feature selection method widely applied in complicated biological problems. This algorithm selected a subset of 20 features having the most correlation with the class (relevance) and the least correlation between themselves (redundancy).

This feature subset was further selected by multivariate logistic least absolute shrinkage and selection operator (LASSO) regression. LASSO is a shrinkage method that can actively select from a large and potentially multicollinear set of variables in the regression, resulting in a more relevant and interpretable set of predictors [25]. LASSO performs via a continuous shrinking operation, minimizing regression coefficients to reduce the likelihood of overfitting, forcing, and producing coefficients that are exactly 0, thus selecting the nonzero variables to remain in the model. For the LASSO regression, we used cross-validation to select the most appropriate  $\lambda$ . The remained nonzero features in LASSO regression would be used to build the radiomics model. The calculating result of the radiomics model was named "radiomics score" and was combined with important factors of the clinical model to build a new combined model. The comparison of the area under the curve (AUC) of these models was done by Delong's test.

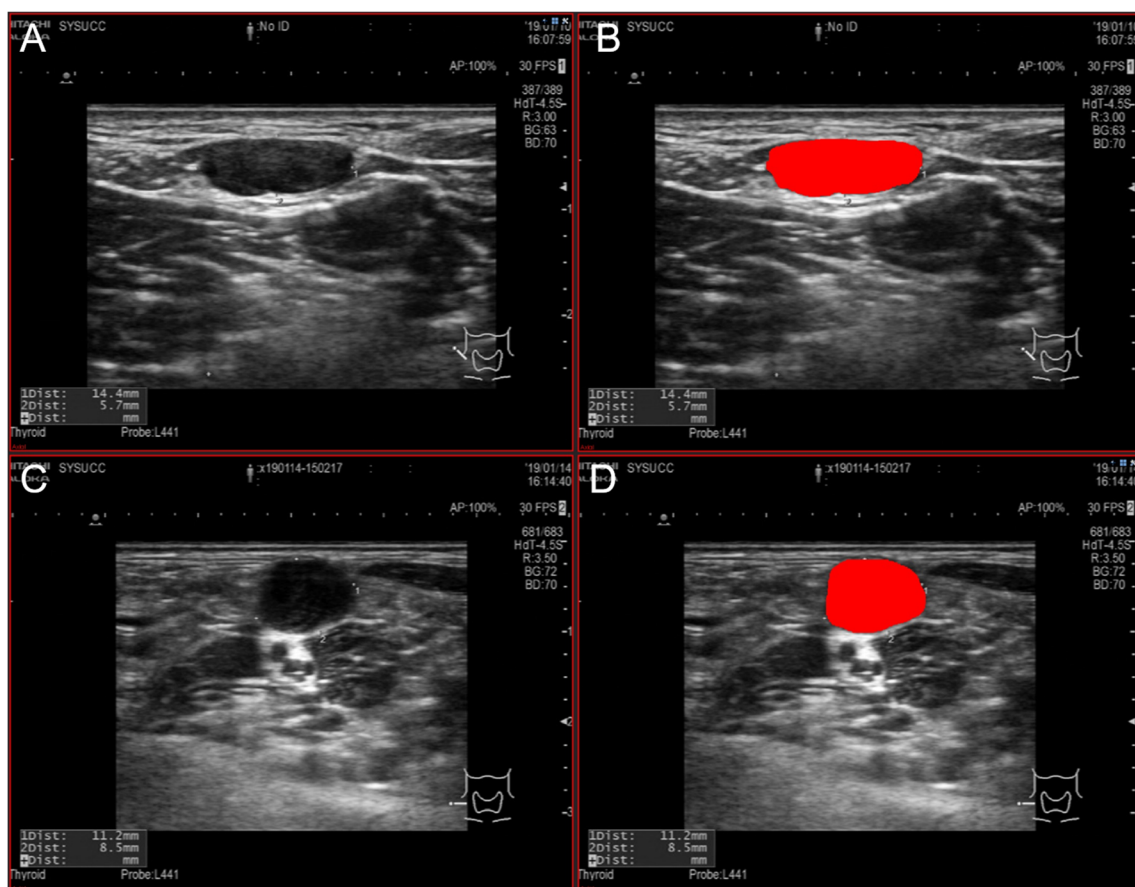


**Fig. 2** Example of delineating region of interest (ROI) on grayscale US images. **A** The original grayscale image of a benign CLN enrolled. **B** The CLN outline was delineated as the ROI of the lymph node. **C, D** The original grayscale image and ROI of a metastatic CLN enrolled

## Statistical analysis

Data were presented as number (%) or mean  $\pm$  SD/median as approximate. The receiver operating characteristic (ROC) curves were performed to determine the performance of the models; and accuracy, sensitivity, specificity, and AUC were calculated. All statistical analyses for the present study were performed with R v3.4.1 and Python v3.5.6. A two-tailed  $p$  value  $< 0.05$  indicated statistical significance.

## Results

### Patient characteristics

A total of 1866 patients with clinical suspicious cervical lymph nodes underwent core-needle biopsy in 2019 in our center (Fig. 1). All of these patients were evaluated by an ultrasound doctor with at least 5-year experience, and lymph nodes with suspicious ultrasound signs would undergo a biopsy. After excluding patients with other malignant tumor metastasis and unclear pathological diagnosis, ultrasound images of 695 patients were carefully reviewed. Images of poor

quality were excluded. Finally, 284 cases of benign lymph node diseases and 205 cases of NPC CLNM were enrolled. Benign lymph node diseases included chronic inflammation, reactive lymphoid hyperplasia, granulomatous inflammation, and histiocytic necrotizing lymphadenitis. General ultrasound characteristics of these lymph nodes were shown in Table 1. The CLNM group had a larger male ratio (70.7% vs 52.5%,  $p < 0.001$ ), and younger age (median age 47 vs 52,  $p = 0.005$ ). Most of these lymph nodes were oval-shaped with clear edges. About 90% of metastases were in the upper neck region. They were larger ( $p < 0.001$ ) and rounder in shape ( $p = 0.035$ ), and had a higher ratio of unclear hilus ( $p < 0.001$ ) than those in the benign group.

### Model developing and validation

The demographic characteristics and general US features were analyzed by univariate logistics regression (Table 2). Characteristics with  $p$  value  $< 0.05$  were included in multivariate logistics regression. After multivariate logistics regression analysis, lymph nodes in the upper neck, larger long axis, and unclear hilus remained significant factors for CLNM ( $p < 0.001$ ). The AUCs of the training and validation dataset were

**Table 1** Clinicopathologic characteristics and general ultrasound features in the training and testing groups

Characteristics	Benign	NPC metastasis	<i>p</i>	$\chi^2$
Gender	284	205	< 0.001	16.57
Male	149 (52.5%)	145 (70.7%)		
Female	135 (47.5%)	60 (29.3%)		
Age	52 (39, 61)	47 (39, 54)	0.002	
Long axis (mm)	14 (11, 19)	23 (16, 29)	< 0.001	
Short axis (mm)	7 (6, 9)	12 (10, 16)	< 0.001	
Long/short axis ratio	2.0 (1.5, 2.4)	1.8 (1.6, 2.1)	0.035	
Lymph node level*			< 0.001	100.22
Upper neck	130 (45.8%)	184 (89.8%)		
Lower neck	154 (54.2%)	21 (10.2%)		
Shape			0.112	4.38
Oval-shape	251 (88.4%)	178 (86.8%)		
Round	17 (6.0%)	7 (3.4%)		
Irregular	16 (5.6%)	20 (9.8%)		
Lymph node edge			0.479	0.50
Clear	275 (96.8%)	196 (95.6%)		
Blur	9 (3.2%)	9 (4.4%)		
Hilus			< 0.001	12.62
Clear	66 (23.2%)	22 (10.7%)		
Unclear	218 (76.8%)	183 (89.3%)		

\* Lymph node level was divided into the upper neck (above the cricoid cartilage, including level Ia, Ib, II, III, Va, and pretracheal region), and the lower neck (below the cricoid cartilage, including level IV, Vb, prelaryngeal region, and supraclavicular region)

0.841 (0.798–0.884) and 0.838 (0.776–0.901), respectively (Table 5) (Fig. 4A, B).

A total of 386 features were extracted from the grayscale images, including first-order features, shape features, and textural features. Stability analysis of radiomics features evaluated the ICC of these features and identified 264 relevantly stable features with ICC > 0.75. A subset of the top 20 features with low redundancy and high relevance were obtained from

these radiomics features using the mRMR algorithm. This subset was further analyzed by LASSO regression. Finally, the number of features was reduced to 7 (Table 3) (Fig. 3). A multivariate logistics regression model was developed based on these features, with AUCs of 0.808 (0.762–0.854) in the training dataset and 0.810 (0.739–0.881) in the validation dataset (Table 5) (Fig. 4A, B). There was no significant difference in the AUC between the clinical and radiomics models in the training dataset ( $p = 0.781$ ) or the validation dataset ( $p = 0.435$ ).

The radiomics score of every lymph node image was calculated by the radiomics model we built. A combined model was developed by integrating the radiomics score and clinical predictors, and a nomogram based on this model was developed (Fig. 4F). In the combined model, the location of the suspicious lymph node, the long axis, the state of hilus, and the radiomics score were all independent predictors of CLNM of NPC (Table 4). As shown in Fig. 4, the AUCs of the combined model were significantly larger than those of the clinical model in both the training dataset (0.864 vs 0.841,  $p = 0.049$ ) and the validation dataset (0.880 vs 0.838,  $p = 0.027$ ) (Table 5). The calibration curve showed the predicted lymph node status by the combined model was very close to the actual results in both datasets (Fig. 4C). The decision curve analysis (DCA) curves also revealed the improvement of the combined model in both datasets (Fig. 4D, E).

## Discussion

Among the imaging methods, ultrasound is considered a convenient and effective method for assessing cervical lymph nodes and performs excellently in the diagnosis of metastatic lymph nodes in cancers such as thyroid cancer and head and neck cancer [26, 27]. However, current diagnostic MRI criteria for NPC metastatic CLN include only lymph node minimum diameter, central necrosis or a contrast-enhanced rim, nodal grouping, and extranodal neoplastic spread

**Table 2** Univariate and multivariate logistic regression of general ultrasound factors

Characteristics	Univariate		Multivariate	
	OR (95% CI)	<i>p</i>	OR (95% CI)	<i>p</i>
Male	1.99 (1.27, 3.13)	0.003	1.40 (0.80, 2.45)	0.235
Age	0.99 (0.97, 1.00)	0.102		
Upper neck	8.16 (4.67, 14.26)	< 0.001	5.42 (2.92, 10.08)	< 0.001
Long axis	1.16 (1.12, 1.2)	< 0.001	1.13 (1.08, 1.18)	< 0.001
Short axis	1.19 (1.12, 1.26)	< 0.001	1.01 (0.98, 1.05)	0.539
Long/ short axis ratio	0.73 (0.52, 1.03)	0.071		
Unclear hilus	2.40 (1.30, 4.45)	0.005	4.54 (2.12, 9.71)	< 0.001



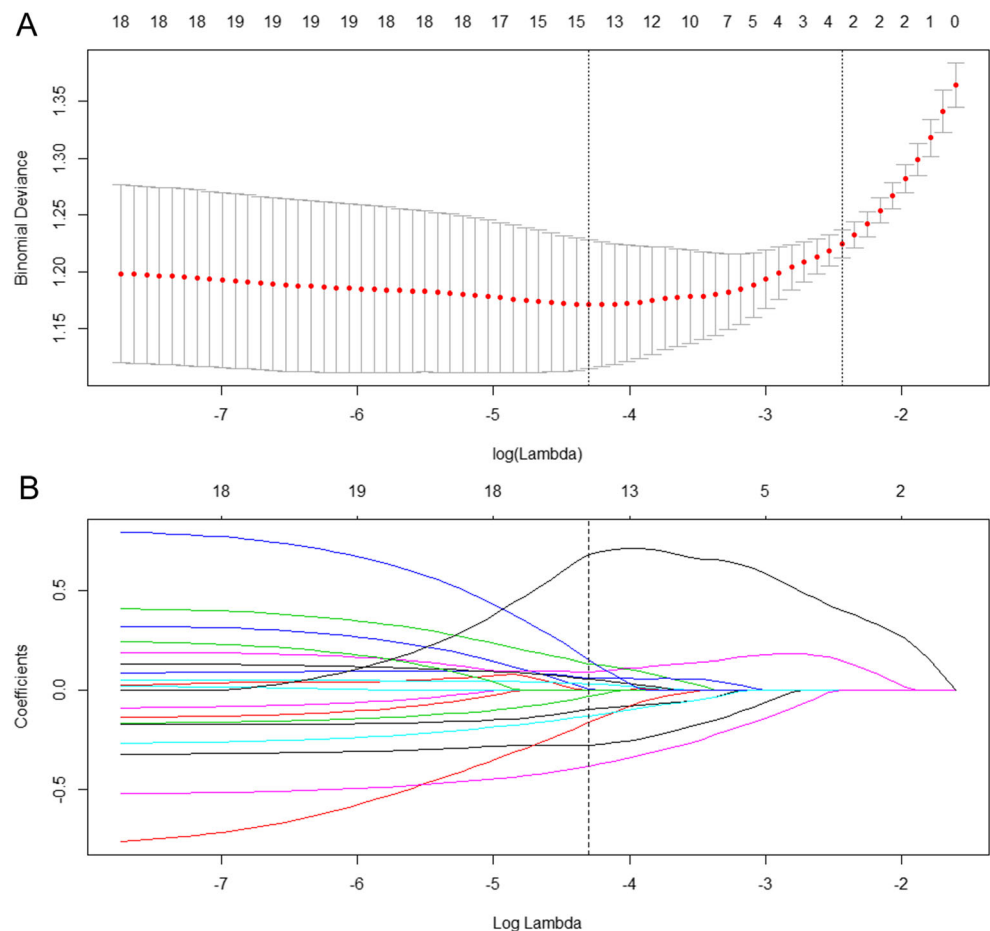
**Table 3** Multivariate logistic regression model of radiomics factors

Features	OR (95% CI)	<i>p</i>
original_glm_ClusterProminence	0.70 (0.51–0.95)	0.022
original_glm_Idn	1.38 (0.97–1.96)	0.074
original_firstorder_Kurtosis	0.51 (0.25–1.01)	0.054
original_glszm_LargeAreaHighGrayLevelEmphasis	1.59 (0.94–2.68)	0.082
original_firstorder_Minimum	0.69 (0.49–0.96)	0.026
lbp_3D_m2_firstorder_10Percentile	0.56 (0.41–0.78)	< 0.001
original_shape_MinorAxisLength	2.16 (1.42–3.29)	< 0.001

(ENS), which makes it difficult to diagnose CLNM involving nontypical lymph nodes, or differentiate from benign lymph node diseases with necrosis or hyperplasia, such as tuberculosis and histiocytic necrotizing lymphadenitis [15, 28, 29]. This may lead to a false-positive diagnosis. Several studies proved that omitting the lower neck during irradiation in node-negative NPC was safe and feasible [30, 31], but a false-positive diagnosis would turn these patients into full neck irradiation.

Radiomics, based on extracting amounts of data through high-throughput medical imaging, can transform images into

measurable features for further objective and quantitative analysis of the biological characteristics of diseases. Studies have shown that image feature-based radiomics extraction has objective characteristics and great value in predicting clinical outcomes in many diseases, such as thyroid cancer, lung cancer, liver cancer, and breast cancer [19–22]. Radiomic models based on MRI, CT, and PET/CT were developed to predict the treatment response of patients with NPC [32–34]. This correlation provides the possibility of building a radiomics model based on medical images to diagnose CLNM in NPC. Therefore, in this study, we focused on the clinical value of

**Fig. 3** Figures of logistic LASSO regression. **A** Cross-validation plot for the penalty term. **B** Lasso path plot of the model in the training dataset

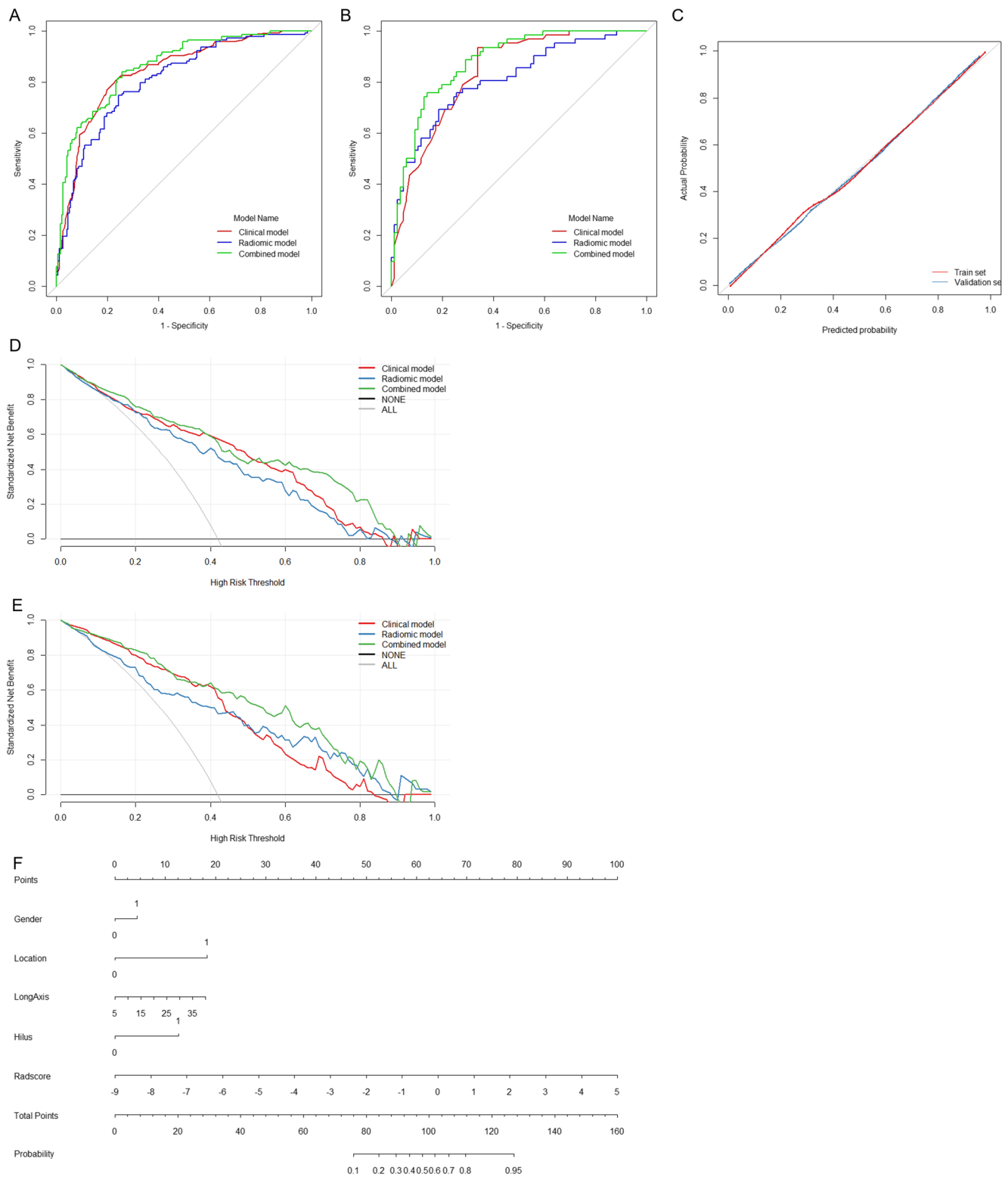


**Fig. 4** Results of the multivariate logistic regression model. **A** Receiver operating characteristic (ROC) curve of the training dataset. **B** ROC curves of the validation dataset. **C** The calibration curve of the combined

model. **D** The decision curve analysis (DCA) figure of the three models of the training dataset. **E** The DCA figure of the three models of the validation dataset. **F** Nomograph based on the combined model

ultrasound radiomics features in the diagnosis of CLNM in NPC.

Texture features are microscopic features that are difficult to be recognized by the naked eye and thus difficult to apply in

**Table 4** Multivariate logistic regression model combining clinical factors and the radiomics model

Characteristics	OR (95% CI)	<i>p</i>
Male	1.55 (0.87–2.78)	0.137
Upper neck	6.13 (3.29–12.12)	< 0.001
Long axis	1.05 (1.00–1.11)	0.048
Unclear Hilus	3.58 (1.64–7.83)	0.001
Radiomics score	2.05 (1.48–2.85)	< 0.001

clinical practice. However, with radiomics analysis, these quantitative features can be detected and integrated for CLNM prediction. In recent years, studies have shown that radiomics could effectively predict lymph node metastasis for cancer patients based on quantitative image features derived from routine US images [20, 35]. Therefore, US radiomics signatures have the potential to be noninvasive biomarkers for the preoperative assessment of CLN status in NPC. In the present study, we developed and validated noninvasive radiomics models based on cervical lymph node characteristics to predict CLNM in nasopharyngeal carcinoma. Minor axis length was reserved after LASSO regression and remains a significant factor in the final model, which is consistent with the current diagnosis guidelines. The combined prediction model for CLNM demonstrated favorable discrimination and yielded AUCs of 0.864 and 0.880 in the training and validation dataset, respectively.

In this study, lymph nodes selected for the benign disease group were those that had suspicious imaging findings but pathologically proved to be benign. These lymph nodes should be evaluated by two ultrasound doctors, and a biopsy would be performed only if the two doctors reached a consensus. Ultrasound diagnosis can be subjective because it relies on the experience of doctors. But naked eyes can only evaluate macroscopic features of the images, which makes it difficult to distinguish metastatic lymph nodes from some hyperplasia lymph nodes caused by inflammation or infection. Radiomics provides a quantitative evaluation of microscopic features of the ultrasound images, to make full use of image

information and maximize benefits. The present study indicated the potential value of radiomics analysis based on gray-scale ultrasound in the diagnosis of cervical lymph node metastasis. It helps distinguish benign lymph nodes with suspicious macroscopic image features. Studies proved that SWE can help discriminate between malignant and benign lymph nodes with satisfactory sensitivity and specificity [36]. A combination of SWE and radiomics may further improve the diagnosis efficiency. Based on this information, radiomics analysis has promising value in the prediction of CLNM in NPC by ultrasound. Previous studies proved the association between the involvement of CLNM and retropharyngeal lymph node (RLN) [37]. Results of neck US examination in NPC patients may be suggestive of RLN status.

However, the present study has several limitations. Firstly, this study was a single-center retrospective study. Secondly, benign lymph node diseases were diagnosed in different backgrounds (patients with and without NPC). Thirdly, the image acquisition was performed on different US machines and under different acquisition conditions. This may be good for the robustness of the model but increased the difficulty of image analysis. Fourthly, compared with that of the clinical model, although the AUC improvement of the combined model was statistically significant, it was low. This might be due to the fact that only gray-scale images were analyzed and a limited patient number was included in this study. Images from other new techniques such as shear-wave elastography and contrast-enhanced ultrasound were also proved to be effective in the diagnosis of CLNM and can be included in further study [36, 38]. In the future, multi-center prospective studies with more patients enrolled are needed to improve the performance of the model in discriminating between malignant and benign cervical lymph nodes for NPC patients.

## Conclusion

In conclusion, ultrasound radiomics analysis has potential value in screening meaningful ultrasound features and improving

**Table 5** Performance of logistic model in the train and validation datasets

Model	Training dataset				Validation dataset			
	AUC (95%CI)	ACC	Sp	Se	AUC (95%CI)	ACC	Sp	Se
Clinical	0.841 (0.798–0.884)	0.783	0.758	0.818	0.838 (0.776–0.901)	0.777	0.663	0.935
Radiomic	0.808 (0.762–0.854)	0.754	0.758	0.748	0.810 (0.739–0.881)	0.736	0.756	0.710
Combined	0.864 (0.825–0.902) <sup>+</sup>	0.783	0.742	0.839	0.880 (0.826–0.933) <sup>+</sup>	0.777	0.698	0.887

ACC, accuracy; Sp, specificity; Se, sensitivity

<sup>+</sup>, *p* < 0.05 in DeLong's test



diagnostic efficiency in NPC patients with CLNM. Nevertheless, multimodal ultrasound imaging and multicenter studies with a larger dataset are needed to further improve the performance of the model.

**Funding** The authors state that this work has not received any funding.

## Declarations

**Guarantor** The scientific guarantor of this publication is Jianhua Zhou.

**Conflicts of interest** The authors of this manuscript declare no relationships with any companies whose products or services may be related to the subject matter of the article.

**Statistics and biometry** No complex statistical methods were necessary for this paper.

**Informed consent** Written informed consent was waived by the IRB for this retrospective study.

**Ethical approval** This retrospective study was approved by the Institutional Review Board (IRB) of Sun Yat-sen University Cancer Center.

## Methodology

- retrospective
- diagnostic study
- performed at one institution

## References

1. Chen Y-P, Chan ATC, Le Q-T, Blanchard P, Sun Y, Ma J (2019) Nasopharyngeal carcinoma. *Lancet* 394:64–80
2. Ho FCH, Tham IWK, Earnest A, Lee KM, Lu JJ (2012) Patterns of regional lymph node metastasis of nasopharyngeal carcinoma: a meta-analysis of clinical evidence. *BMC Cancer* 12:98
3. Lee AW, Ma BB, Ng WT, Chan AT (2015) Management of nasopharyngeal carcinoma: current practice and future perspective. *J Clin Oncol* 33:3356–3364
4. Jiang C, Gao H, Zhang L et al (2020) Distribution pattern and prognosis of metastatic lymph nodes in cervical posterior to level V in nasopharyngeal carcinoma patients. *BMC Cancer* 20:667
5. Huang CL, Chen Y, Guo R et al (2020) Prognostic value of MRI-determined cervical lymph node size in nasopharyngeal carcinoma. *Cancer Med* 9:7100–7106
6. Yin X, Lv L, Pan XB (2020) Prognosis of extracapsular spread of cervical lymph node metastases in nasopharyngeal carcinoma. *Front Oncol* 10:523956
7. Ng S-H, Chang JT-C, Chan S-C et al (2004) Nodal metastases of nasopharyngeal carcinoma: patterns of disease on MRI and FDG PET. *Eur J Nucl Med Mol Imaging* 31:1073–1080
8. Chen W-S, Li J-J, Hong L, Xing Z-B, Wang F, Li C-Q (2016) Comparison of MRI, CT and 18F-FDG PET/CT in the diagnosis of local and metastatic of nasopharyngeal carcinomas: an updated meta analysis of clinical studies. *Am J Transl Res* 8:4532–4547
9. Gupta A, Rahman K, Shahid M et al (2011) Sonographic assessment of cervical lymphadenopathy: role of high-resolution and color Doppler imaging. *Head Neck* 33:297–302
10. Richards PS, Peacock TE (2007) The role of ultrasound in the detection of cervical lymph node metastases in clinically N0 squamous cell carcinoma of the head and neck. *Cancer Imaging* 7:167–178
11. Li Y, Su X, Yao F, Wu T, Peng J, Yang A (2021) Comparison of the value of ultrasound and enhanced magnetic resonance imaging in judging cervical lymph node metastasis in patients with oral cancer. *Bull Cancer* 108:1085–1090
12. Kim K, Shim S-R, Lee S-W, Kim S-J (2021) Diagnostic values of F-18 FDG PET or PET/CT, CT, and US for preoperative lymph node staging in thyroid cancer: a network meta-analysis. *Br J Radiol* 94:20201076
13. Chen B-B, Li J, Guan Y et al (2018) The value of shear wave elastography in predicting for undiagnosed small cervical lymph node metastasis in nasopharyngeal carcinoma: a preliminary study. *Eur J Radiol* 103:19–24
14. Nie J, Ling W, Yang Q, Jin H, Ou X, Ma X (2020) The value of CEUS in distinguishing cancerous lymph nodes from the primary lymphoma of the head and neck. *Front Oncol* 10:473
15. Moon IS, Kim DW, Baek HJ (2015) Ultrasound-based diagnosis for the cervical lymph nodes in a tuberculosis-endemic area. *Laryngoscope* 125:1113–1117
16. Park S, Kim JY, Ryu YJ, Lee H (2021) Kikuchi cervical lymphadenitis in children: ultrasound differentiation from common infectious lymphadenitis. *J Ultrasound Med* 40:2069–2078
17. Lambin P, Rios-Velazquez E, Leijenaar R et al (2012) Radiomics: extracting more information from medical images using advanced feature analysis. *Eur J Cancer* 48:441–446
18. Aerts HJWL, Velazquez ER, Leijenaar RTH et al (2014) Decoding tumour phenotype by noninvasive imaging using a quantitative radiomics approach. *Nat Commun* 5:4006
19. Jiang M, Li C, Tang S et al (2020) Nomogram based on shear-wave elastography radiomics can improve preoperative cervical lymph node staging for papillary thyroid carcinoma. *Thyroid* 30:885–897
20. Zheng X, Yao Z, Huang Y et al (2020) Deep learning radiomics can predict axillary lymph node status in early-stage breast cancer. *Nat Commun* 11:1236
21. Chetan MR, Gleeson FV (2021) Radiomics in predicting treatment response in non-small-cell lung cancer: current status, challenges and future perspectives. *Eur Radiol* 31:1049–1058
22. Mao B, Ma J, Duan S, Xia Y, Tao Y, Zhang L (2021) Preoperative classification of primary and metastatic liver cancer via machine learning-based ultrasound radiomics. *Eur Radiol* 31:4576–4586
23. Robbins KT, Clayman G, Levine PA et al (2002) Neck dissection classification update: revisions proposed by the American Head and Neck Society and the American Academy of Otolaryngology-Head and Neck Surgery. *Arch Otolaryngol Head Neck Surg* 128:751–758
24. van den Brekel MW, Stel HV, Castelijns JA et al (1990) Cervical lymph node metastasis: assessment of radiologic criteria. *Radiology* 177:379–384
25. Tibshirani R (1997) The lasso method for variable selection in the Cox model. *Stat Med* 16:385–395
26. Bryson TC, Shah GV, Srinivasan A, Mukherji SK (2012) Cervical lymph node evaluation and diagnosis. *Otolaryngol Clin North Am* 45:1363–1383
27. Nishio N, Fujimoto Y, Hiramatsu M et al (2019) Diagnosis of cervical lymph node metastases in head and neck cancer with ultrasonic measurement of lymph node volume. *Auris Nasus Larynx* 46:889–895

28. Amin MB, Greene FL, Edge SB et al (2017) The Eighth Edition AJCC Cancer Staging Manual: continuing to build a bridge from a population-based to a more "personalized" approach to cancer staging. *CA Cancer J Clin* 67:93–99
29. Yang J-S, Du Z-X (2019) Comparison of clinical and pathological features of lymph node tuberculosis and histiocytic necrotizing lymphadenitis. *J Infect Dev Ctries* 13:706–713
30. Xiao F, Dou S, Li Y et al (2019) Omitting the lower neck and sparing the glottic larynx in node-negative nasopharyngeal carcinoma was safe and feasible, and improved patient-reported voice outcomes. *Clin Transl Oncol* 21:781–789
31. Tang LL, Tang XR, Li WF et al (2017) The feasibility of contralateral lower neck sparing intensity modulation radiated therapy for nasopharyngeal carcinoma patients with unilateral cervical lymph node involvement. *Oral Oncol* 69:68–73
32. Yan C, Shen D-S, Chen X-B et al (2021) CT-based radiomics nomogram for prediction of progression-free survival in locoregionally advanced nasopharyngeal carcinoma. *Cancer Manag Res* 13:6911–6923
33. Xu H, Liu J, Huang Y, Zhou P, Ren J (2021) MRI-based radiomics as response predictor to radiochemotherapy for metastatic cervical lymph node in nasopharyngeal carcinoma. *Br J Radiol* 94: 20201212
34. Peng H, Dong D, Fang M-J et al (2019) Prognostic value of deep learning PET/CT-based radiomics: potential role for future individual induction chemotherapy in advanced nasopharyngeal carcinoma. *Clin Cancer Res* 25:4271–4279
35. Yu J, Deng Y, Liu T et al (2020) Lymph node metastasis prediction of papillary thyroid carcinoma based on transfer learning radiomics. *Nat Commun* 11:4807
36. Heřman J, Sedláčková Z, Fürst T et al (2019) The role of ultrasound and shear-wave elastography in evaluation of cervical lymph nodes. *Biomed Res Int* 2019:4318251
37. Liu L-Z, Zhang G-Y, Xie C-M, Liu X-W, Cui C-Y, Li L (2006) Magnetic resonance imaging of retropharyngeal lymph node metastasis in nasopharyngeal carcinoma: patterns of spread. *Int J Radiat Oncol Biol Phys* 66:721–730
38. Chen L, Chen L, Liu J, Wang B, Zhang H (2020) Value of qualitative and quantitative contrast-enhanced ultrasound analysis in preoperative diagnosis of cervical lymph node metastasis from papillary thyroid carcinoma. *J Ultrasound Med* 39:73–81

**Publisher's note** Springer Nature remains neutral with regard to jurisdictional claims in published maps and institutional affiliations.

Springer Nature or its licensor holds exclusive rights to this article under a publishing agreement with the author(s) or other rightsholder(s); author self-archiving of the accepted manuscript version of this article is solely governed by the terms of such publishing agreement and applicable law.